Quantifying the Uncertainty in Deterministic Phonon Transport Calculations of Thermal Conductivity using Polynomial Chaos Expansions

Jackson R. Harter,[†] P. Alex Greaney,[*] Todd S. Palmer[†]

[†]*Department of Nuclear Science and Engineering, Oregon State University*
[*]*Department of Mechanical Engineering and MS&E Program, University of California - Riverside*
harterj@oregonstate.edu, agreaney@engr.ucr.edu, palmerts@engr.orst.edu

INTRODUCTION

The nature of computational simulations requires the inclusion of an uncertainty analysis, as we have limited knowledge of all physically determined input parameters for a computationally simulated problem. We rely on uncertainty quantification (UQ) to characterize our confidence in the outcomes. Quantifying uncertainty can provide a basis for certifications in high-consequence decisions, such as nuclear reactor design, and is a fundamental component of model validation.

We employ a previously developed method of uncertainty quantification, polynomial chaos expansion with stochastic collocation (PCE-SC) [1], applied to deterministic phonon transport simulations. In these simulations, we use the neutron transport code Rattlesnake [2], which solves the Self-Adjoint Angular Flux (SAAF) formulation of the transport equation with a continuous finite element (CFEM) spatial discretization and discrete ordinates, spherical harmonics angular discretizations. Rattlesnake was developed in the multi-physics object oriented simulation environment (MOOSE) framework [3]. We have previously shown Rattlesnake to be effective in simulating phonon transport [4].

We aim to provide a deterministic phonon transport framework for heterogeneous nuclear fuel with fission product defects to predict thermal conductivity (κ) [5]. A first principles, physics-based calculation of thermal conductivity must involve factors such as the microstructure of nuclear fuel, which constantly changes during the fission process through the formation of isotopic decay products. Heat transport in oxide nuclear fuels is dominated by phonon transport. Impurities in the bulk material influence the transport of energy at the fundamental level, altering the scattering behavior of phonons and electrons.

Conventionally, heat transport follows classical physics based on the heat equation derived from Fourier's law

$$\boldsymbol{q} = -\kappa \boldsymbol{\nabla} T, \tag{1}$$

where $\boldsymbol{q}$ is heat flux, κ is thermal conductivity and $\boldsymbol{\nabla} T$ is a temperature gradient. However, Fourier's law is a macroscopic empirical law in which the thermal conductivity κ does not have a mechanistic connection to the underpinning heat transport processes. Thermal conductivity of a material depends both on the material's intrinsic ability to transport heat and a variety of resistive effects caused by defects in the material. Thus *ab initio* prediction of the macroscopic conductivity — the property of interest for safe reactor operation — requires simulating detailed processes of heat transport, and then determining the *effective* thermal conductivity of the simulated material from the resulting heat flux under the imposed temperature difference. The thermal conductivity of a bulk, homogeneous, dielectric material can be well estimated by the mechanistically derived expression [6]:

$$\kappa_{\text{bulk}} = \frac{1}{3} C_v v_g \lambda, \tag{2}$$

where C_v, v_g, and λ are the volumetric specific heat, phonon speed, and phonon mean free path, respectively.

The importance of microstructure and boundary scattering is illustrated by Fig. 1, which shows the reduction in the effective thermal conductivity across a thin slab of material (Fig. 2) as compared to its bulk value. In these problems the relevant parameter is the material's *acoustic thickness*, its characteristic distance L relative to the phonon mean free path λ [7]. In Eq. (2) the largest source of uncertainty is λ. While propagating uncertainty in λ to uncertainty in κ through Eq. (2) is trivial, systems with extrinsic scattering require more sophisticated approaches. At the microscopic level, uncertainty in λ changes both a material's intrinsic thermal conductivity and its acoustic thickness.

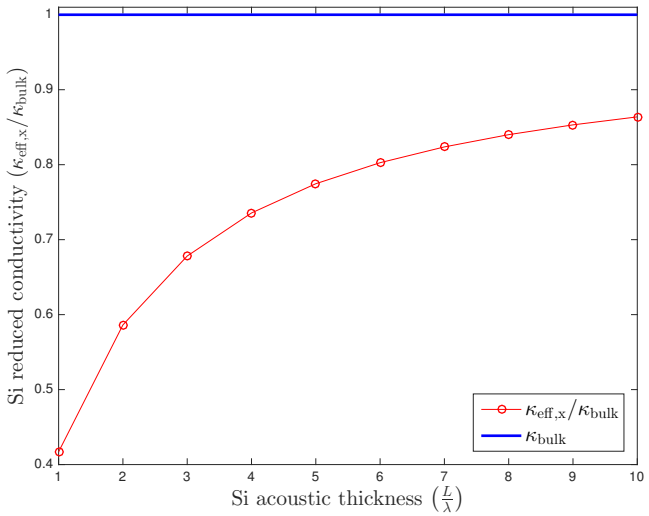

Fig. 1. Reduction in the thermal conductivity across a thin slab of material as compared to bulk.

Our goal is to propagate the uncertainty in λ through the determinstic transport computation of κ. Because there are a small number of uncertain input quantities, we use the method of polynomial chaos expansion (PCE), which expresses solutions in the form of spectral expansions of an uncertain variable [1]. This approach combines both intrusive and non-intrusive methods of uncertainty propagation techniques and results in a unique formulation which is very effective and efficient for problems with few uncertain parameters [8, 9].

We use PCE-SC to measure propagation of uncertainty in a 3-D phonon transport problem of homogeneous silicon, to compute the mean and variance in temperature, heat flux and thermal conductivity.

METHODS

Brute force Monte Carlo can be used to calculate statistical moments of various relevant quantities from realizations of statistical distributions of input parameters, though it can be prohibitively slow because of the Central Limit Theorem. PCE-SC approximates integrals over the probability distributions using deterministic quadrature, and has been shown to be very computationally efficient for small numbers of uncertain input parameters.

We solve the steady-state Boltzmann transport equation (BTE) to determine the radiant intensity of heat-carrying phonons and from the moments of the intensity, determine the effective thermal conductivity. The governing equation is the BTE for gray phonons in the SAAF formulation (which we have developed previously [5]) using the single mode relaxation time approximation [6], given by Eq. (3):

$$-\lambda\hat{\boldsymbol{\Omega}}\cdot\boldsymbol{\nabla}\left[\lambda\hat{\boldsymbol{\Omega}}\cdot\boldsymbol{\nabla}I\left(\boldsymbol{r},\hat{\boldsymbol{\Omega}}\right)\right]+I\left(\boldsymbol{r},\hat{\boldsymbol{\Omega}}\right)=-\lambda\hat{\boldsymbol{\Omega}}\cdot\boldsymbol{\nabla}I^{0}\left(\boldsymbol{r}\right)+I^{0}\left(\boldsymbol{r}\right) \quad (3)$$

Here, $I(\boldsymbol{r},\hat{\boldsymbol{\Omega}})$ is phonon radiant intensity at position $\boldsymbol{r}\,(x,y,z)$ traveling in direction $\hat{\boldsymbol{\Omega}}$. The radiance I has units of $\mathrm{W}\cdot\mathrm{m}^{-2}\cdot\mathrm{sr}^{-1}$. In this transport problem, the change in the phonon intensity at a point has two contributions: a streaming term from the spatial variation in intensity, and a collision term due to the deviation of the radiance from the equilibrium phonon radiance $I^{0}(\boldsymbol{r})$. The mean free path λ is the product of phonon speed v_g and relaxation time τ and has units of length (m).

The zeroth angular moment of phonon radiance I is proportional to temperature, phonon speed, and volumetric specific heat capacity:

$$\int_{4\pi} I\left(\boldsymbol{r},\hat{\boldsymbol{\Omega}}\right)d\Omega=\frac{C_v v_g T}{4\pi}. \quad (4)$$

The first angular moment is the heat flux:

$$\boldsymbol{q}\left(\boldsymbol{r}\right)=\int_{4\pi} I\left(\boldsymbol{r},\hat{\boldsymbol{\Omega}}\right)\hat{\boldsymbol{\Omega}}\,d\Omega \quad (5)$$

In a cube of silicon with side length 3λ (Fig. 2), we simulate a 1 K temperature gradient along the x-axis, with boundary temperatures of $T_R = 301\,\mathrm{K}$, $T_L = 300\,\mathrm{K}$, $C_v = 1.65\cdot10^{6}\,\mathrm{J}\cdot\mathrm{m}^{-3}\cdot\mathrm{K}^{-1}$, $v_g = 8430\,\mathrm{m}\cdot\mathrm{s}^{-1}$. Simulations use the generalized minimal residual (GMRES) method [10] to solve the linear system, with solver convergence criteria of $\epsilon = 10^{-6}$. The finite element mesh is constructed in CUBIT and is composed of 10^3 elements, and the simulation has ~10^4 degrees of freedom. The run-time is approximately 7 seconds on a 2.8 GHz Intel i7 CPU with 16 GB RAM. The reported mean free path for phonons in silicon at room temperature (300 K) varies widely [11, 12]. Reported values of λ are averaged values that coalesce the scattering behavior of a broad spectrum of phonon wavelengths and their interactions with different types of extrinsic defects. The volumetric specific heat C_v and phonon speed v_g can be determined with good accuracy from first principles, while λ is often obtained as a fitting parameter needed to make Eq. (2) match some empirically determined value of κ. The large variation in measured κ means that applying an empirically obtained λ from one problem to another is accompanied by a large degree of uncertainty, justifying the need for UQ for these types of problems.

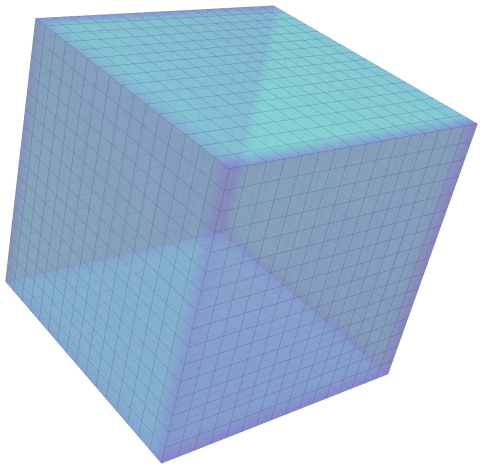

Fig. 2. Mesh of silicon domain with side length 3λ.

In this study, we have assigned a relative uncertainty on λ of 33% $\left(\frac{1}{3}\right)$ based on literature values of mean free path in silicon [11, 12], and so choose its range to be $\lambda \pm \lambda/3$. We assume that the statistical distribution for λ is uniform, such that

$$\lambda\left(\Xi\right)=\bar{\lambda}+\frac{\bar{\lambda}}{3}\Xi, \qquad \Xi\in(-1,1)\,, \quad (6)$$

The uniform distribution evaluated at the ordinates of an S_8 Gauss-Legendre quadrature is shown in Fig. 3. [Other statistical distributions are possible in the PCE-SE approach.]

In PCE-SC we express the randomness introduced in the intensity (and its angular moments) as an expansion in orthogonal polynomials. The uniform statistical distribution is most efficiently treated with Legendre polynomials and Gauss quadrature. Each quantity of interest in the transport simulation has a statistical distribution and is expanded in terms of a finite series of Legendre polynomials in the random variable. The expansion for temperature, for example, becomes

$$T\left(\Xi\right)\approx\sum_{\ell=0}^{N}T_\ell P_\ell\left(\Xi\right), \quad (7)$$

where P_ℓ is the Legendre polynomial of order ℓ and T_ℓ is the expansion coefficient. For this work, Legendre polynomial order was set to $N = 8$, with quadrature order set to $M = 8$. An S_8 Gauss-Legendre quadrature will exactly integrate polynomials up to order 7.

The BTE is solved for each of the discrete values of λ associated with the chosen quadrature, and numerical integrals are performed to estimate the statistical moments of the temperature (zeroth angular moment of I) via

$$T_\ell\left(\boldsymbol{r}\right)\approx\frac{2\ell+1}{2}\sum_{\ell=0}^{N}\sum_{m=1}^{M}w_m T_\ell\left(\boldsymbol{r},\Xi_m\right)P_\ell\left(\Xi_m\right). \quad (8)$$

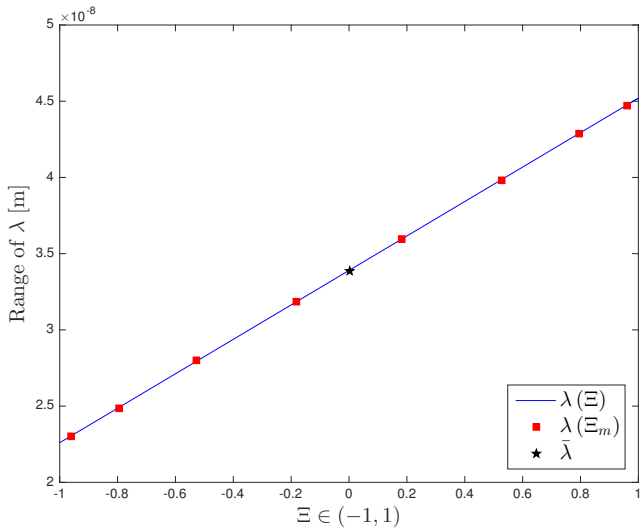

Fig. 3. The continuous ($\lambda(\Xi)$) statistical mean free path distribution and the values of λ corresponding to the S_8 Gauss quadrature ($\lambda(\Xi_m)$). $\bar{\lambda}$ is the value of the phonon mean free path [13].

[An analogous equation exists for the heat flux $\boldsymbol{q}$.]

Once the moments have been obtained through Eq. (8), the mean and variance may be computed. The mean temperature at each spatial location is equal to zeroth Legendre moment of the temperature distribution:

$$\langle T(\boldsymbol{r})\rangle = T_0(\boldsymbol{r}). \tag{9}$$

The variance in temperature can be computed from the remaining Legendre moments:

$$\sigma_T^2(\boldsymbol{r}) = \sum_{\ell=1}^{N} \frac{1}{2\ell+1} T_\ell^2(\boldsymbol{r}) \tag{10}$$

From the statistical mean and variance of $\boldsymbol{q}(\boldsymbol{r})$ and the temperature gradient across the axis of transport, we are able to compute a volume-averaged thermal conductivity, $\langle \kappa_{\text{eff,x}} \rangle$, as

$$\langle \kappa_{\text{eff,x}} \rangle = -\frac{\int d^3r\, \boldsymbol{e}_x \cdot \boldsymbol{q}(\boldsymbol{r})}{\Delta T/L}. \tag{11}$$

Values for all output quantities are reported in Table I.

TABLE I. Mean and standard deviation for $\langle q_\rangle$, $\langle T\rangle$, $\langle \kappa_{\text{eff,x}}\rangle$

$\langle q_{\text{x}}\rangle \left(\frac{\text{W}}{\text{m}^2}\right)$	$\langle T_{\text{x}}\rangle$ (K)	$\langle \kappa_{\text{eff,x}}\rangle \left(\frac{\text{W}}{\text{m·K}}\right)$
-1.05 ± 0.14	300.5 ± 0.01	107.5 ± 14.2

RESULTS AND ANALYSIS

Temperature is calculated at each spatial location x_i, and is a function of C_v, v_g and I. Figure 4 contains the spatial distribution of temperature for the mean free path associated with each of the quadrature points.

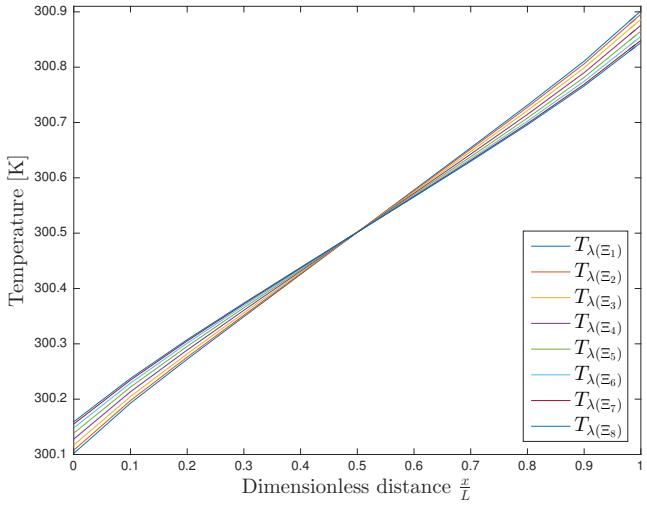

Fig. 4. Spatial temperature distributions for each λ computed from the chosen quadrature.

Figure 5 shows the mean and standard deviation of temperature at each location x_i along the domain. The uncertainty in the center goes to zero due to symmetry of the problem. σ_T is highest at the boundaries, and is a function of the acoustic thickness of the problem. As the acoustic thickness increases, the radiant sources at the boundaries shift from ballistic to diffuse scattering regimes. In an acoustically thin medium, where $L \approx \lambda$, phonons leaving a colder boundary are in the ballistic scattering regime, and propagate far across the medium to reach the hotter boundary causing the material temperature to be smaller than that associated with the prescribed incident intensity. In an acoustically thick medium, where phonons are in the diffuse scattering regime, this effect is significantly diminished. These are boundary scattering effects, and are well characterized in simulations of phonon transport [7, 13].

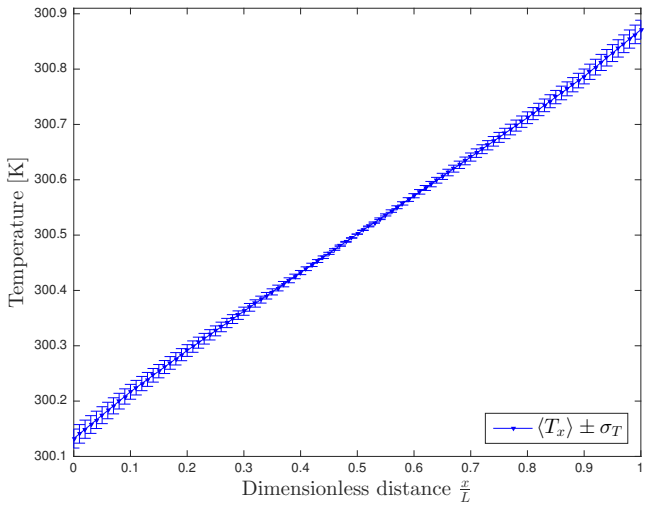

Fig. 5. Mean and standard deviation of temperature along x-axis of silicon.

Mean values of T, q and κ over the spatial domain along with their associated standard deviations ($\pm \max|\sigma|$) are re-

ported in Table I. We expect $\langle T_x \rangle$ to be approximately the midpoint average of the boundary temperatures due to the homogeneity of the problem.

The equilibrium heat flux is constant over the spatial domain, however, the same boundary effects which influenced the temperature distribution also materialize in q, which elevate the values of q near the domain boundaries. This effect may be responsible for the inflated uncertainty in q, which is higher than expected. The uncertainty in q propagates into the calculation of σ_κ

The value of $\langle \kappa_{\text{eff,x}} \rangle$ is in good agreement with κ_{eff} at an acoustic thickness of 3λ, roughly 68% of the value of $\kappa_{\text{bulk}} = 157\,\text{W}\cdot\text{m}^{-1}\cdot\text{K}^{-1}$ given by Eq. (2). Figure 6 compares $\kappa_{\text{eff.x}}$ at many acoustic thicknesses normalized to κ_{bulk} and $\langle \kappa_{\text{eff,x}} \rangle$ with its associated standard deviation. Thermal conductivity has a strong dependence on acoustic thickness of the medium at the nanoscale, this relationship is made clear in Fig. 6.

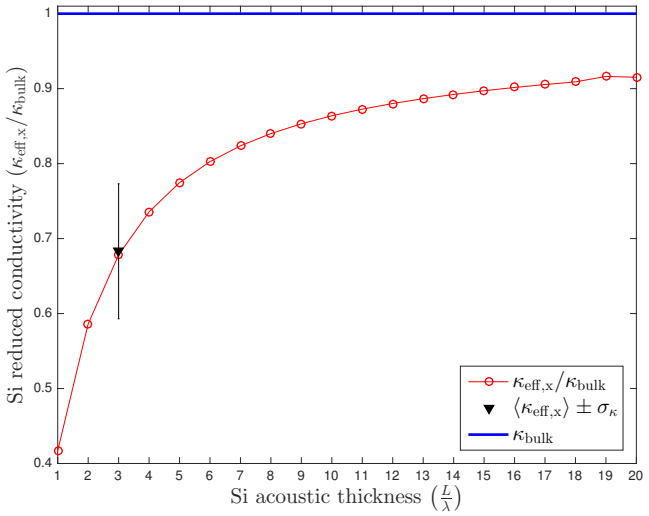

Fig. 6. κ_{eff} normalized to κ_{bulk} for varying acoustic thicknesses, $\langle \kappa_{\text{eff,x}} \rangle$ and σ_κ.

CONCLUSIONS

We have shown the PCE-SC method to be effective in providing uncertainty quantification for a deterministic phonon transport simulation. This method is accurate and efficient for simulations with few uncertain variables. The phonon mean free path is our uncertain variable, and this uncertainty is projected into the solutions of the phonon transport equation which yield $\langle q \rangle$, which in turn yields $\langle \kappa_{\text{eff}} \rangle$; the uncertainty in $\langle \kappa_{\text{eff}} \rangle$ is proportional to the uncertainty in $\langle q \rangle$. The variation in λ influences the acoustic thickness and thermal conductivity. We intend to broaden the application of PCE-SC to our heterogeneous phonon transport simulations. Parametric studies could be performed to measure the accuracy in using different orders for the Gaussian quadrature and chaos expansions, in addition to performing Monte Carlo studies to show an efficiency comparison. The deterministic sampling aspect of the PCE-SC method is very useful in simulations with a small number of uncertain parameters and is beneficial in providing UQ analysis to deterministic phonon transport simulations.

ACKNOWLEDGMENTS

This work was supported by Idaho National Laboratory and XSEDE.

REFERENCES

1. D. XIU and G. E. KARNIADAKIS, "The Wiener-Askey Polynomial Chaos for Stochastic Differential Equations," *SIAM Journal of Scientific Computing*, **24**, 619–644 (2002).
2. Y. WANG, H. ZHANG, and R. MARTINEAU, "Diffusion Acceleration Schemes for Self-Adjoint Angular Flux Formulation with a Void Treatment," *Nuclear Science and Engineering*, **176**, 201–225 (2014).
3. D. GASTON, C. NEWMAN, G. HANSEN, and D. LEBRUN-GRANDIE, "MOOSE: A Parallel Computational Framework for Coupled Systems of Nonlinear Equations," *Nuclear Science and Engineering*, **239**, 1768–1778 (2009).
4. J. HARTER, P. A. GREANEY, and T. PALMER, "Characterization of Thermal Conductivity using Deterministic Phonon Transport in Rattlesnake," *Transactions of the American Nuclear Society*, **112**, 829–832 (2015).
5. J. HARTER, *Predicting Thermal Conductivity in Nuclear Fuels using Rattlesnake-Based Deterministic Phonon Transport Simulations*, Master's thesis, Oregon State University (2015).
6. J. ZIMAN, *Electrons and Phonons: The Theory of Transport Phenomena in Solids*, Oxford University Press (2001).
7. A. MAJUMDAR, "Microscale heat conduction in dielectric thin films," *Journal of Heat Transfer*, **115**, 7–16 (1993).
8. E. FICHTL and A. PRINJA, "The stochastic collocation method for radiation transport in random media," *Journal of Quantitative Spectroscopy & Radiative Transfer*, **112**, 646–659 (2011).
9. S. DULLA, A. PRINJA, and P. RAVETTO, "Random effects on reactivity in molten salt reactors," *Annals of Nuclear Energy*, **64**, 353–364 (2014).
10. Y. SAAD and M. SCHULTZ, "GMRES: A Generalized Minimal Residual Algorithm for Solving Nonsymmetric Linear Systems," *SIAM Journal of Scientific Computing*, **7**, 856–869 (1986).
11. G. ROMANO and J. GROSSMAN, "Heat Conduction in Nanostructured Materials Predicted by Phonon Bulk Mean Free Path Distribution," *Journal of Heat Transfer*, **137** (2015).
12. P. MAREPELLI, J. MURTHY, B. QIU, and X. RUAN, "Quantifying Uncertainty in Multiscale Heat Conduction Calculations," *Journal of Heat Transfer*, **136** (2014).
13. B. YILBAS and S. BIN MANSOOR, "Phonon Transport in Two-Dimensional Silicon Thin Film: Influence of Film Width and Boundary Conditions on Temperature Distribution," *European Physical Journal B*, **85**, 234–242 (2012).